

**Immunomodulatory Properties of 1,2-Dihydro-4-hydroxy-2-oxo-1,8-naphthyridine-3-carboxamide Derivative VL15.**

Anna Maria Malfitano\*, Chiara Laezza†, Simone Bertini‡, Daniela Marasco§, Tiziano Tuccinardi‡, Maurizio Bifulco\*, Clementina Manera‡

\*Dipartimento di Medicina e Chirurgia, Università di Salerno, Fisciano, Salerno.

† Istituto di Endocrinologia e Oncologia Sperimentale, IEOS, CNR, Napoli, Italy.

‡ Dipartimento di Farmacia, Università di Pisa, via Bonanno 6, 56126 Pisa, Italy.

§Department of Pharmacy, University of Naples "Federico II", 80134 Napoli, Italy

Correspondence: Anna Maria Malfitano and Clementina Manera

[amalfitano@unisa.it](mailto:amalfitano@unisa.it), [clementina.manera@farm.unipi.it](mailto:clementina.manera@farm.unipi.it)

## **Abstract**

1,2-dihydro-4-hydroxy-2-oxo-1,8-naphthyridine-3-carboxamide derivative VL15 has been recently developed as a selective cannabinoid CB2 receptor compound. Given the high selectivity of this compound at the cannabinoid CB2 receptor and the well-known protective function of this receptor in neurological disorders with autoimmune component like multiple sclerosis, we assessed the immunomodulatory properties of VL15. We assessed on activated peripheral blood mononuclear cells (PBMC), proliferation and viability, cell cycle progression and measured activation markers and the expression of phosphorylated proteins. We found that VL15 reduces PBMC proliferation slightly affecting cell vitality, blocks the cells cycle progression and down-regulates the levels of T cell activation markers as well as the expression of phosphorylated proteins, NF- $\kappa$ B, IKK $\alpha\beta$ , IKB $\alpha$ , ERK and Akt. VL15 was also used in drug-permeability assays on Caco-2 cell line to evaluate its oral bioavailability and on MDCKII-hMDR1 cell lines to estimate its propensity to cross the blood-brain barrier by passive diffusion, in order to potentially maintain its efficiency on the infiltrating auto-reactive lymphocytes in the central nervous system (CNS). In these models, VL15 showed high intestinal absorption and good BBB penetration. Our findings suggest that VL15, by controlling the immune response, might find potential application as orally administered drug in pathologies like multiple sclerosis.

**Keywords:** immunomodulation, intestinal absorption, blood-brain barrier diffusion, cannabinoid CB2 receptor, 1,8-naphthyridine-3-carboxamide derivative, neurodegeneration.

## 1.1 Introduction

Numerous studies have investigated the biological role of the endocannabinoid system (ECS) and its regulatory functions in health and disease. The ECS consists of the G-protein coupled cannabinoid receptors, the endogenous ligands anandamide (AEA) and 2-arachidonoylglycerol (2-AG), and the enzymes responsible for endocannabinoid biosynthesis, cellular uptake and metabolism. To date, two major cannabinoid receptors, CB1 and CB2 have been described [1, 2]. The CB1 receptor is preferentially expressed in the central nervous system (CNS) [3, 4, 5], the CB2 receptor is predominantly expressed by immune cells [6], although some reports showed its presence in the CNS [7, 8, 9]. Increasing reports suggest a major physiological function of the ECS in the regulation of bone growth [10], pain [11], cancer [12, 13], and psychiatric disorders [14]. ECS plays a role also in immune-mediated diseases of the CNS such as multiple sclerosis (MS), which results in focal areas of inflammation containing immune cell infiltrates and demyelination [15]. The beneficial effects of cannabinoid derived-drugs in MS have been reported [11, 16, 17]. In the brain, the anti-inflammatory and neuro-protective effects of cannabinoid receptor agonists have been demonstrated in animal models of MS, Alzheimer's disease (AD), stroke and amyotrophic lateral sclerosis (ALS) [18, 19]. For example, in a viral model of MS, CB1 receptor agonists have been shown to reduce perivascular CD4+T lymphocytes infiltration, inhibit microglial responses and suppress the up-regulation of adhesion molecules in the brain endothelium [20]. However, the use of CB1 receptor agonists has a limited therapeutic potential [21] because many adverse psychoactive effects are mediated by the CB1 receptor, thus emerging proposals support as alternative strategy, to focus on selective CB2 receptor agonists because of their minimal binding to CB1 receptors and therefore devoid of psychotropic effects. Recently, new compounds like 1,8-naphthyridine derivatives [22, 23, 24, 25, 26], endowed with higher CB2 affinity and selectivity versus CB1, have been developed. Some of these compounds showed pharmacological properties like inhibitory action on immunological human basophil activation [22, 23], anti-proliferative activity [26] and we recently demonstrated their effects on immune cells isolated from multiple sclerosis patients [27]. In a recent study, we showed that some 1,8-naphthyridine derivatives modulate the immune response but possess a medium intestinal absorption and blood-brain barrier (BBB) diffusion [28]. The use of CB2 receptor selective compounds showing immune-modulatory properties, might be of potential interest in neurological diseases with autoimmune component like multiple sclerosis (MS), especially if these drugs can

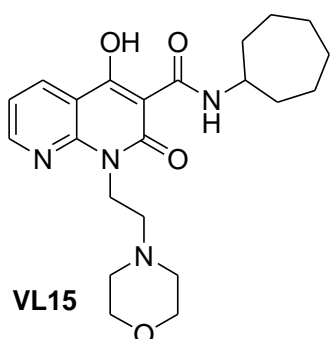
efficiently cross the BBB to elicit their effects on the auto-reactive cells of the CNS, since unrelated or not totally related to the CB1 mediated psychoactivity. In this study, we tested the potential immunomodulatory effects of 1,2-dihydro-4-hydroxy-2-oxo-1,8-naphthyridine-3-carboxamide derivative VL15 [26] in human peripheral blood mononuclear cells (PBMC) isolated from healthy donors and its properties of diffusion in Caco-2 and MDCKII-hMDR1 cell lines. Caco-2 cell line is cellular model of the intestinal epithelial barrier and MDCKII-MDR1 cell line was identified as a model for quality predictions of BBB passive diffusion, which was used to evaluate CNS penetration of CB1 antagonists [29]. Furthermore, some physico-chemistry properties were calculated for a better understanding of its ability to cross cell barriers. We have previously developed this compound on the basis of the 1,8-naphthyridin-2(1*H*)-one scaffold and showed a remarkable CB2 receptor affinity and selectivity ( $K_i = 1.8$  nM;  $K_i(\text{CB1})/K_i(\text{CB2}) = 130$ ), indeed we demonstrated CB2 receptor activity of this compound in tumor cell lines mediated by the CB2 receptor [26]. In this study, we show that VL15 exerts anti-proliferative effects associated with inhibition of the cytokine tumor necrosis factor (TNF)  $\alpha$ , block of the cell cycle and down-regulation of T cell activation markers. Furthermore, VL15 reduces NF-kB, IKK $\alpha\beta$ , IKB $\alpha$ , ERK, and Akt expression levels. Notably, VL15 shows higher intestinal absorption and BBB penetration by passive diffusion with respect to a previously tested compound [28]. Our data suggest the possible application of this compound as novel immune-suppressive and anti-inflammatory agent and its potential effects on the CNS.

## 2.2 Materials and Methods

### 2.2.1 Drugs

1,2-dihydro-4-hydroxy-2-oxo-1,8-naphthyridine-3-carboxamide derivative, VL15 (N-cycloheptyl-4-hydroxy-1-(2-morpholin-4-ylethyl)-2-oxo-1,2-dihydro-1,8-naphthyridine-3-carboxamide) [26] and reference compounds (caffeine, cimetidine and amprenavir) were dissolved in dimethyl sulfoxide (DMSO). The chemical structure of VL15 is reported in Fig.1.

**Fig. 1**



### *2.2.2 Isolation of human PBMC*

At the University Hospital “Federico II” of Naples we recruited all volunteers that provided written informed consent in agreement with the Declaration of Helsinki to the research use of their residual buffy coats. We isolated PBMC from buffy coats of healthy donors as previously described [30]. For the experiments we used RPMI 1640 (Life Technologies, Paisley, UK) supplemented with 2mM L-glutamine (Life Technologies), penicillin/streptomycin (Life Technologies), and 10% heat-inactivated FBS (Sigma Chemical Co., St Louis, MO, USA).

### *2.2.3 Proliferation assays on human PBMC*

We cultured PBMC derived from healthy subjects ( $1 \times 10^5$  cells per well) in triplicate in round-bottomed 96-well plates in 200  $\mu$ l of RPMI 10% FBS (final volume). We added human myelin basic protein (MBP) (10  $\mu$ g/ml) (Sigma) to stimulate the cells. We added VL15 to the MBP-stimulated PBMC to get final concentrations of 0.3, 1, 3 and 10  $\mu$ M. Cells were incubated for 6 days and then were pulsed for 18 h with 1  $\mu$ Ci of  $^3$ H-thymidine (Amersham-Pharmacia Biotech, Cologno Monzese, Milano, Italy). After the incubation, PBMC were harvested on glass-fiber filters using a Tomtec (Orange, CT) 96-well cell harvester, and counted in a 1205 Betaplate liquid scintillation counter (Wallac, Gaithersburg, MD).

### *2.2.4 TNF- $\alpha$ production.*

After 48 h of incubation of PBMC activated with MBP in the presence and in the absence of VL15, we harvested supernatants from the cell cultures to analyze TNF- $\alpha$  release at concentration of VL15 of 10 $\mu$ M and 3  $\mu$ M. Tests were performed by Human Fluorokine Multianalyte profiling (MAP) Base Kit (R&D system).

### *2.2.5 Cell viability assays.*

In the presence and in the absence of VL15 at 10 $\mu$ M, we cultured PBMC with MBP (10 $\mu$ g/ml) in 24-well plates. After 6 days of incubation, PBMC were stained with trypan blue and counted by microscopy.

### *2.1.6 Sulphorhodamine B cytotoxicity assay.*

We evaluated as previously described [31] protein content and drug cytotoxicity by sulphorhodamine B assay. We cultured for 48 h Chinese hamster ovary (CHO) cells ( $2 \times 10^4$  cells per well) in the presence and in the absence of our drug.

#### *2.2.7 Flow cytometry assays.*

We analyzed cell cycle progression culturing for 6 days PBMC ( $1 \times 10^6$  cells) with MBP (10  $\mu\text{g/ml}$ ) in the presence of the drug (10  $\mu\text{M}$ ) in 24-well plates. We stained with propidium iodide (PI) and processed as previously described [16].  $10^5$  cells from each experimental condition. Then, we analyzed T cell activation markers culturing the cells as above described. We stained  $10^5$  cells from each experimental condition with CD4-Cy-Chrome, CD69-PE, CD54 (ICAM)-FITC, or CD4-Cy-Chrome and CD25-PE, CD49d (VLA-4)-PE, (BD-Bioscience) and incubated for 15 min in the dark at 4 °C. We washed with PBS PBMC and acquired by flow cytometry. Marker analysis was performed on the region of CD4+T lymphocytes and we compared marker expression in treated cells to that of activated and no- treated cells. We used the program Summit v4.3. (Dako) to perform the analyses.

#### *2.2.8 Electrophoresis and immunoblots.*

For the analysis of protein expression, we obtained cell extracts from the culture of MBP activated PBMC treated with VL15 (10  $\mu\text{M}$ ) for 6 days and processed the cells as previously done [32]. We used primary antibodies (1:1000) (host species: rabbit) specific for NF-kB p65 (Cell Signaling Technology Inc., Danvers, MA, USA), IKK $\alpha/\beta$  (Cell signalling), IKB $\alpha$  (Cell signalling), ERK (Cell signaling), Akt (Cell signalling) and their phosphorylated forms: pNF-kB p65 (Cell signalling), pIKK $\alpha/\beta$  (Cell signalling), pIKB $\alpha$  (Cell signalling), pERK (Cell signaling), and pAkt (Cell signalling). Specific proteins were immune-detected with horseradish peroxidase-conjugated donkey anti-rabbit IgG (Bio-Rad, Life Science Research, Hercules, CA, USA), by enhanced chemiluminescence system (ECL) (Amersham GE Healthcare). We used actin (Santa Cruz Biotechnology Inc., anti-rabbit) as control.

#### *2.2.9 Statistical analyses*

Data obtained with assays performed with PBMC and CHO cells were analyzed by ANOVA followed by Bonferroni correction for multiple comparisons; the values statistically significant were P values < 0.05.

### 2.2.10 Caco-2 cellular permeability.

Caco-2 cell line bought from European Collection of Cell Culture (ECACC) was used to test VL15 intestinal absorption. Dulbecco's modified Eagle medium (DMEM), with 10% (v/v) fetal calf serum (FCS), 1% nonessential amino acids (NEAA), *N*-2-hydroxyethylpiperazine-*N'*-2-ethanesulfonic acid (Hepes) buffer 10 mM and a combination of Penicillin (50 U/mL)- Streptomycin (50 µg/ml) was used to culture the cells that were split at confluence with trypsin. Millicell 24-well cell culture plates were used for transport assays. Cells (200,000 cells/well) were incubated at 37 °C and 5% CO<sub>2</sub> for 24 hours, after the incubation, the medium was changed with Enterocyte Differentiation Medium with additives (Becton Dickinson) to allow Caco-2 cells to differentiate within three days. The value of transepithelial electrical resistance (TEER) was >1000 Ω, it was determined by a Millicell-ERS ohm-meter (Millipore). The transport across the Caco-2 monolayer was evaluated from apical to basolateral side (A→B) with the addition of a 10 µM solution of VL15 or of reference compounds (caffeine or cimetidine) in DMEM (1% final concentration of DMSO) to the apical side. The apical, the basolateral side solution and the starting solution were analyzed by LC-MS/MS after 2 hours of incubation at 37 °C, 5% CO<sub>2</sub>. Verapamil was used as internal standard. In order to better mimic the physiological conditions we performed the assays using buffers at different pH (6.5 apical vs. 7.4 basolateral).

### 2.2.11 MDCK-MDR1 cellular permeability

MDCKII-hMDR1 assay was used to test the capacity of VL15 to cross the BBB by passive diffusion. We purchased Madin Darby Canine Kidney cells stably transfected with the human MDR1 gene (MDCKII-hMDR1) by Netherlands Cancer Institute. Dulbecco's modified Eagle medium (DMEM) with 10% (v/v) fetal calf serum (FCS) and a combination of Penicillin (50 U/mL)- Streptomycin (50 µg/ml), was used to growth the cells at 37 °C and 5% CO<sub>2</sub>. Once at confluence, cells were split using trypsin.

Millicell 24-well cell culture plates (EMD Millipore, well cell diameter 12mm, filtration area 0.6 cm<sup>2</sup>) were used for transport studies to seed 100,000 cells/well. Millicell-ERS ohm-meter (Millipore) was used to measure TEER. Monolayers showing values of transepithelial resistance lower than 150 Ω x cm<sup>2</sup> were not considered. The transport across the monolayer was evaluated from apical to basolateral side (A→B) with the addition of a 10 µM solution of VL15 or of reference compounds (caffeine or amprenavir) in DMEM Dulbecco's Phosphate Buffered Saline (DPBS) (0.2% DMSO final concentration) to the apical side. The apical side solution, the basolateral side solution

and the starting solution were analyzed by LC-MS/MS after 1 hour of incubation at 37 °C, 5% CO<sub>2</sub>. Verapamil (0.1 μM) was used as internal standard.

### 2.2.13 Sample analysis

To perform the analyses we used an UPLC (Waters) interfaced with a Premiere XE Triple Quadrupole (Waters). Mobile phases comprised 5% (v/v) acetonitrile in deionized water with 0.1% (v/v) formic acid (Phase A) and 5% (v/v) deionized water in acetonitrile with 0.1% (v/v) formic acid (Phase B). The column was Acquity BEH C18, 50x1mm 1.7 μm at 50 °C with flow of 0.25 ml/min (for intestinal permeability) or of 0.6 ml/min (for BBB permeability) and volume injection of 5 μl. In Table 1 we reported the chromatographic method.

**Table 1.** *Chromatographic method*

<b>Time (min)</b>	<b>%A</b>	<b>%B</b>
0	95	5
0.10	95	<5
0.15	0	100
1.10	0	100
1.15	95	5
1.50	95	5

Samples were analyzed in Multiple Reaction Monitoring conditions (MRM): electron spray ionization (ESI) positive, desolvation temperature 450°C, desolvation gas 900 l/h, cone gas 50 l/h, collision gas 0.22 l/h. In particular for D5 MRM: 394.19 → 281.01, 394.19 → 109.05; Cone Voltage: 32V; Collision Energy: 22-40 eV.

The apparent permeability coefficient (P<sub>app</sub>) (nm x s<sup>-1</sup>), was calculated as follows:

$$P_{app} = dQ_r/dt / A \times C_0$$

dQ<sub>r</sub>/dt is the cumulative amount in the receiver compartment versus time; A the area of the cell monolayer; C<sub>0</sub> the initial concentration of the dosing solution.



The mass balance, i.e. the percentage of the amount of compound found at the end of the experiment (sum of amount in the apical and basolateral chambers) in respect to the amount of compound added at the beginning of the experiment, has been calculated for the compound. Papp of compound showing mass balances less than 60% should be considered underestimated. Papp of compounds showing mass balances more than 140% should be considered overestimated.

#### *2.2.14 Calculated physicochemical properties*

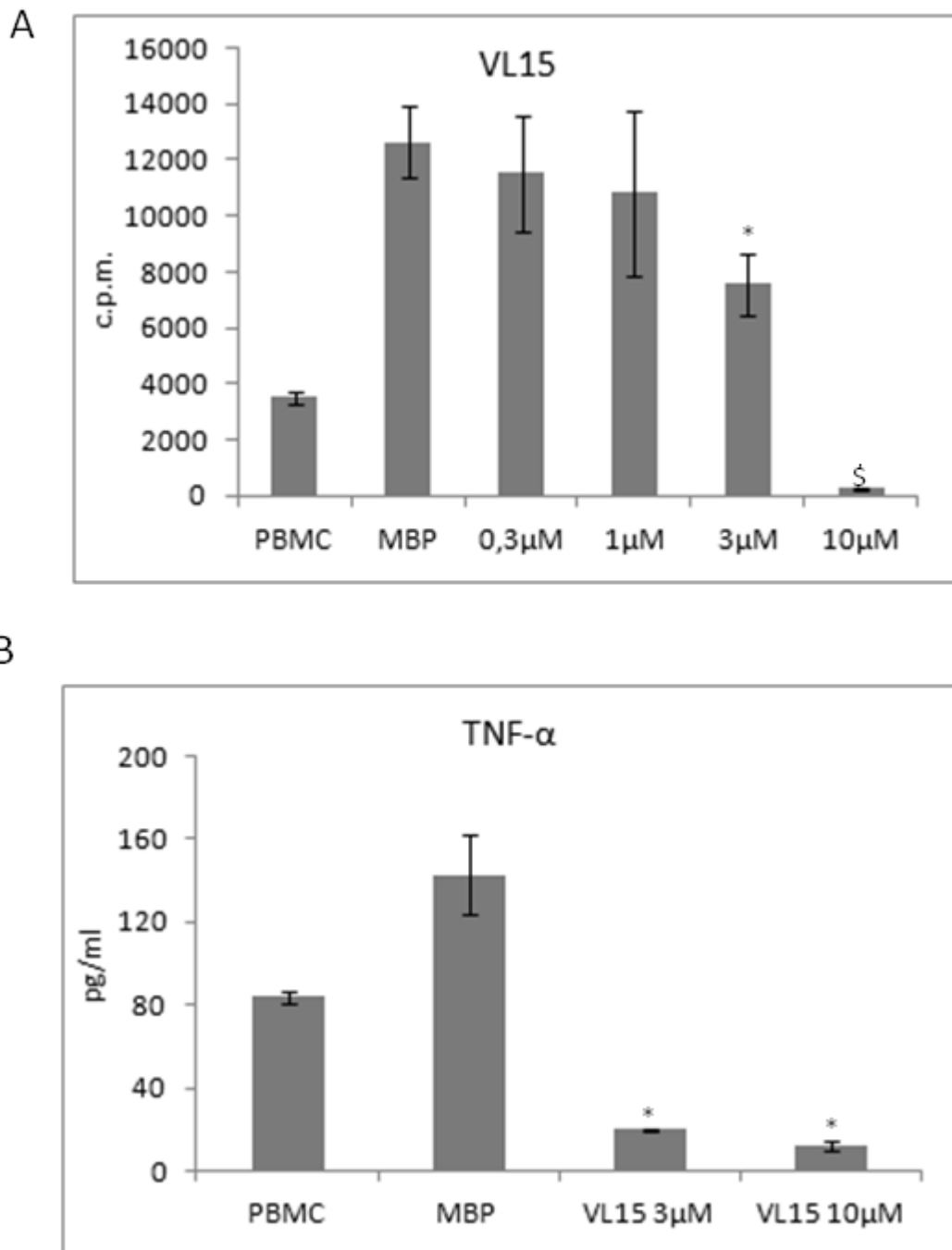
Lipinski parameters, lipophilicity, solubility in water were calculated using QikProp 3.2 [33] Lipophilicity, and water solubility calculations were also carried out using the webbased tool ALOGpS 2.1. [34] Conformational searching using torsional sampling (MCMM) and energy minimization was carried out using the Macromodel module within Maestro modelling package [35]

### **3.3 Results**

#### *3.3.1 VL15 inhibits PBMC proliferation and TNF- $\alpha$ production.*

In order to assess the effect of our compound in immune cells, human PBMC were isolated from buffy coat of healthy donors. MBP activated PBMC were cultured with VL15 at concentrations ranging from 10 to 0,3  $\mu$ M for 6 days. MBP after 6 days of incubation induced proliferation of PBMC with respect to untreated cells (Fig. 2A) and the induced proliferative response was not affected by the vehicle, DMSO used to dissolve the drug (data not shown). VL15 inhibited MBP activated PBMC proliferation at 10  $\mu$ M and 3  $\mu$ M in a dose dependent manner (Fig. 2A). To assess if the anti-proliferative effect of our compound could be associated to the down-regulation of inflammatory cytokine production, we measured the release of TNF- $\alpha$  in cell supernatants. We found that VL15 at 10 $\mu$ M and 3  $\mu$ M was able to significantly decrease MBP-induced TNF- $\alpha$  secretion by PBMC (Fig. 2B).

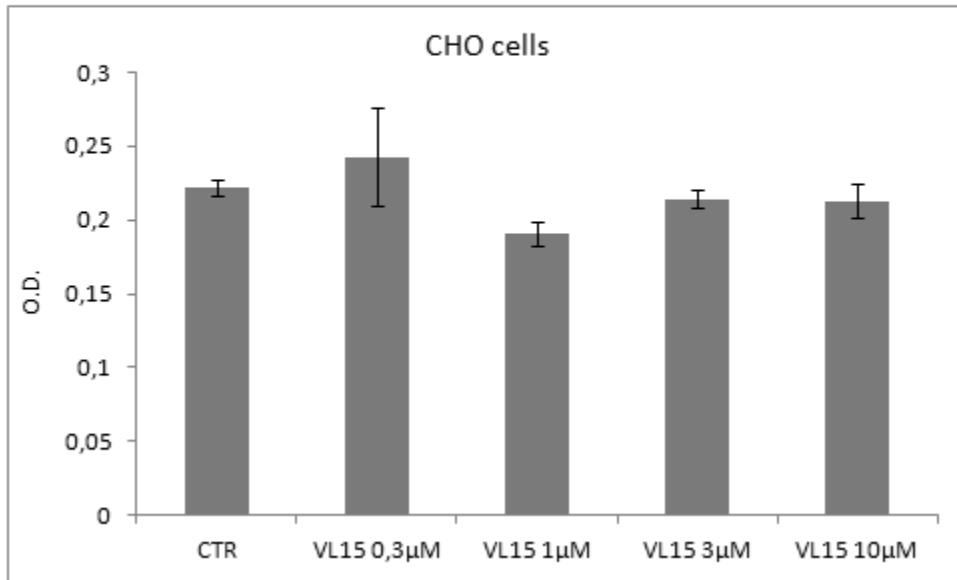
Fig.2



3.3.2 VL15 does not inhibit CHO cell viability.

The effect of VL15 was evaluated on viability and proliferation of cannabinoid receptor deficient CHO cells. VL15 did not block CHO cell proliferation (Fig.3) by sulphorodamine B cytotoxicity test.

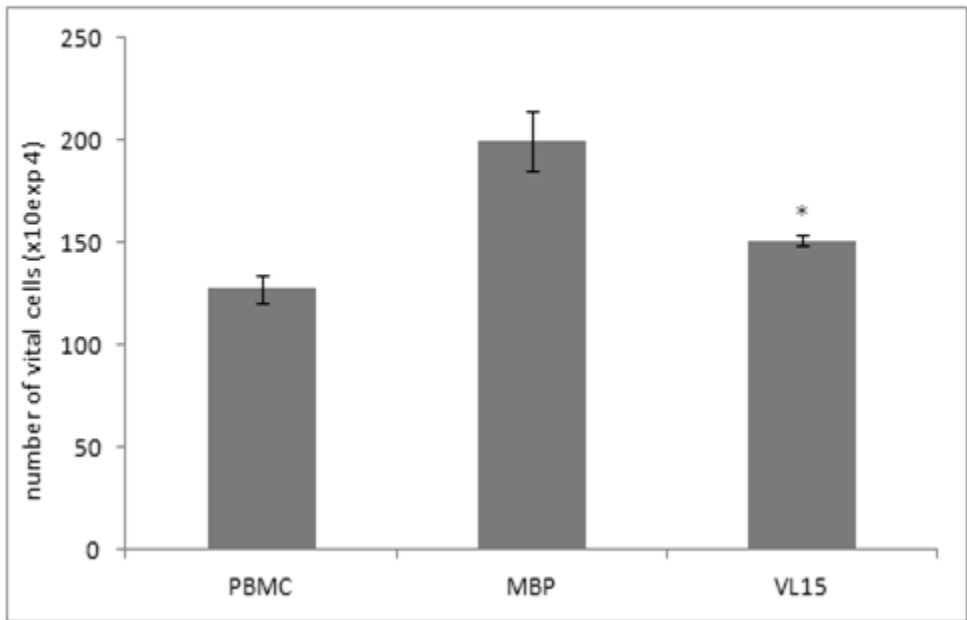
Fig.3



3.3.3 VL15 slightly reduces PBMC viability.

In order to establish if the reported inhibition of proliferation and TNF- $\alpha$  release could be ascribed to cell death rather than to the blocking of a specific cell signaling, we performed viability assays by trypan blue staining. We observed that at the dose of 10 $\mu$ M, VL15 slightly affected viability of PBMC (Fig. 4) with respect to MBP activated cells.

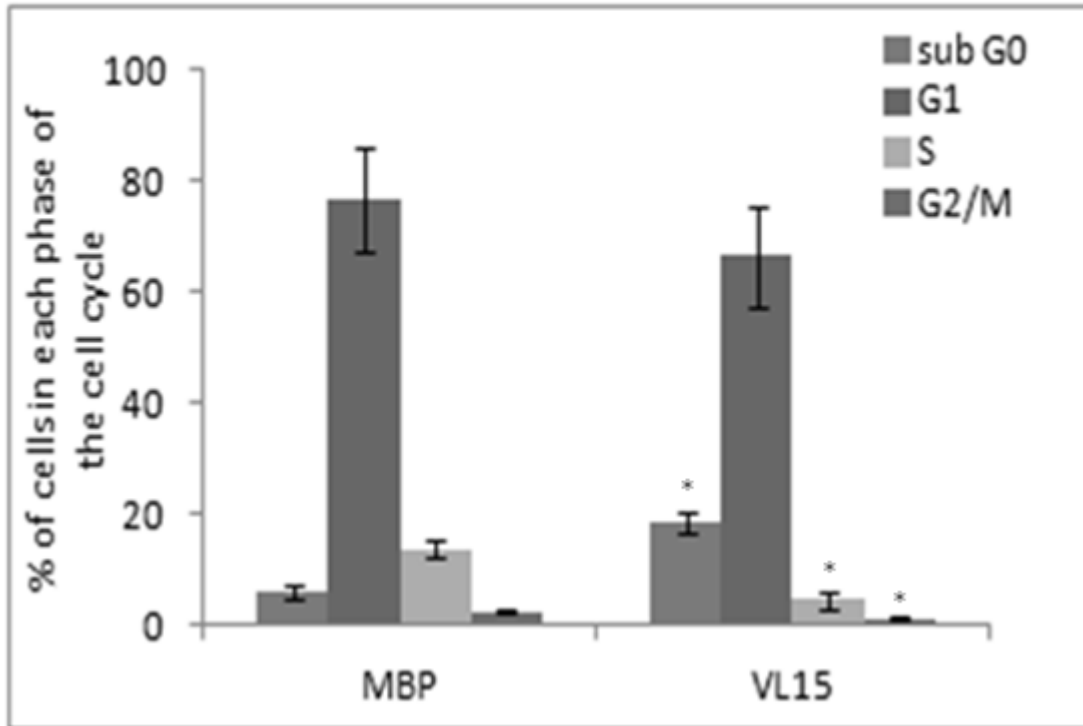
Fig.4



*3.3.4 VL15 controls cell cycle progression of PBMC.*

To establish if the effect observed on cell proliferation was related to modulation of the cell cycle progression, we analyzed the cell cycle following treatment with VL15. We found that VL15 at the concentration of 10 $\mu$ M increased the percentage of cells in the subG0 phase with respect to the control MBP activated cells and decreased the percentage of cells in S phase, also the number of cells in G2/M phase was reduced with respect to the control MBP activated cells (Fig. 5).

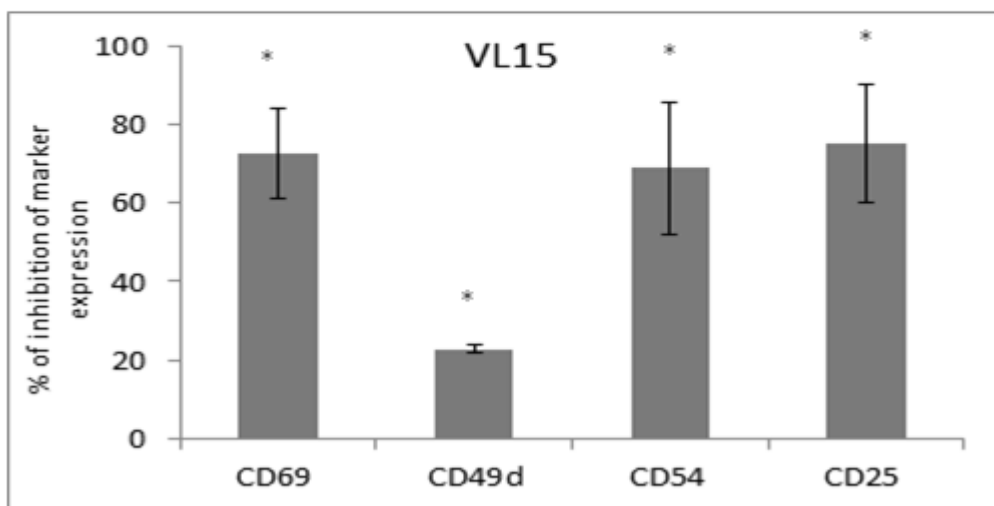
Fig. 5



3.3.5 VL15 inhibits cell surface markers, CD69, CD49d integrin, CD54 adhesion molecule and CD25 on MBP stimulated PBMC.

To establish if the effects detected could be related to block of cell activation, we evaluated the level of T activation markers, CD69 and CD25, the integrin CD49d and the adhesion molecule CD54 in the CD4<sup>+</sup> T cell subset. We observed that VL15 at the concentration of 10 $\mu$ M inhibited the expression of these markers, the effect was less pronounced for CD49d (Fig.6).

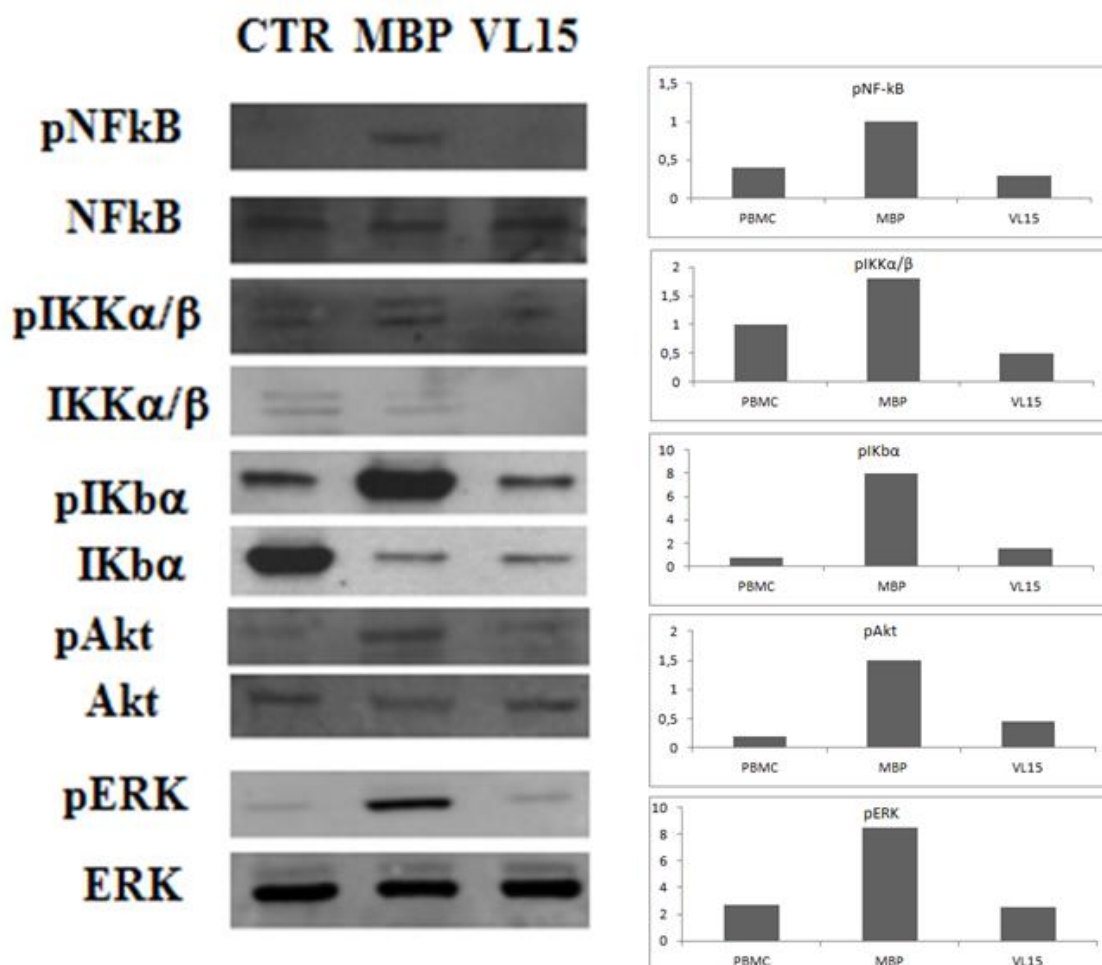
Fig. 6



3.3.6 VL15 regulates NF-kB, IKK $\alpha\beta$ , IKb $\alpha$ , ERK and Akt expression.

Some molecular inflammatory pathways were investigated by evaluation of the expression of phosphorylated and total NF-kB, IKK $\alpha\beta$ , IKb $\alpha$ , ERK and Akt. We observed induction of NF-kB, IKK $\alpha\beta$ , IKb $\alpha$ , ERK, Akt following MBP stimulation with respect to inactivated cells (Fig. 7) and down-regulation of the levels of phosphorylation of NF-kB 65kDa, IKK $\alpha\beta$ , IKb $\alpha$ , ERK and Akt following treatment with VL15 at the concentration of 10  $\mu$ M (Fig. 7).

Fig. 7



### 3.3.7 VL15 exhibits high intestinal permeability and good BBB penetration by passive diffusion

The rank order of Papp for intestinal permeability of VL15 was compared with that of reference compounds tested in the same assay, like caffeine and cimetidine. Papp values <10 nm/s were grouped as ‘low’, ‘medium’ when  $10 \leq Papp \leq 50$  nm/s and ‘high’ when  $Papp > 50$  nm/s. The standard caffeine has a high permeability ( $174.1 \pm 22.3$ ), while cimetidine (Pgp substrate) has a low Papp ( $1.1 \pm 0.1$ ), according to literature and in-house validation data. The Papp A→B value for VL15 was  $125.5 \pm 9.2$  nm/s, indicating high Caco-2 cell permeability. Furthermore, VL15 showed a mass balance value of 48% suggesting that its Papp value could be underestimated. These results indicate that VL15 might possess high absorption from the intestine after oral assumption.

The absorption classification for BBB permeability is: high for  $P_{app} > 150$ ; medium for  $50 \leq P_{app} \leq 150$ ; low for  $P_{app} < 50$ . The used reference compounds were caffeine with high  $P_{app}$  value ( $207.8 \pm 16.6$ ) and amprenavir (P-gp substrate) with low  $P_{app}$  value ( $19.9 \pm 2.5$ ) according to literature and in-house validation data. The  $P_{app}$  A→B value of VL15 was  $97.3 \pm 0.1$  nm/s, indicating medium MDCKII-hMDR1 cell permeability. Furthermore the compound showed a mass balance value of 46% suggesting that its  $P_{app}$  value could be underestimated. These results indicate a good BBB penetration of VL15 by passive diffusion.

### 3.3.8 Physicochemical Characterization

With the aim of better understanding the ability of VL15 to cross cell barriers, some its physico-chemistry properties (LogP, solubility in water and the Lipinski and Jorgensen rules violations ) were calculated. It is common practice to use LogP, the partition coefficient between water and octanol, as a reliable indicator of the lipophilicity of molecules. The computed LogP values (Table 2) were obtained using QikProp [33] and the ‘consensus’ prediction from ALOGPS 2.1 [34] (which obtains the average from values calculated with ALOGPS 2.1, Pharma Algorithms LogP, LogS and pKa, Actelion LogP, COSMOfrag LogP, Molinspiration LogP, KOWWIN LogP and XLOGP programs). As shown in Table 2, compound VL15 has a predicted  $\text{LogP} < 5$  in accordance with Lipinski’s rules; in addition, a low LogP in the range of 0–3 is desirable to reduce toxicity and increase ease of formulation and bioavailability for optimal oral absorption. Aqueous solubility (logS) of organic compounds plays a key impact on many ADME associated properties like uptake, distribution, transport, and ultimately bioavailability. 1,2-dihydro-4-hydroxy-2-oxo-1,8-naphthyridine-3-carboxamide derivative, VL15 is structurally very similar to 4-hydroxy-2-quinolones reported in literature [36,37,38] as slightly acidic compounds with  $pK_a$  values typically in the range 4.2–5.0 which should confer high aqueous solubility in a basic medium.

As shown in Table 1 the compound VL15 shows a logS of -2.0/-2.4, which is in the range of 95% of known drugs [33]. Finally, there is no violations for the Lipinski and Jorgensen rules.



**Table 2.** Calculated lipophilicities (ALOGPs, QPLogP), solubilities (ALOGpS, QPLogS) and rule violations for compound VL15

Property	Value
ALOGPs	1.7
QPLogP	2.3
ALOGpS	-2.4
QPLogS	-2.0
Lipinski Rule of 5 violations	0
Jorgensen Rule of 3 violations	0

#### 4.4 Discussion

Recent studies aimed to develop novel selective CB2 receptor ligands, demonstrated the high CB2 receptor affinity of 1,8-naphthyridine derivatives. Some of these compounds elicited CB2-mediated inhibitory action on immunological human basophil activation, decrease of cell viability in Jurkat leukemia T cell line [23] and exhibited *in vivo* anti-nociceptive effects [25]. In this study, we investigated the immune-modulatory properties of 1,2-dihydro-4-hydroxy-2-oxo-1,8-naphthyridine-3-carboxamide derivative VL15 on human PBMC expressing the CB2 receptor (data not shown) and its potential intestinal absorption and BBB diffusion. We selected this compound since we have previously shown that VL15 is a promising CB2 receptor ligand characterized by high affinity and selectivity for this receptor. We also observed that VL15 exerted anti-proliferative effects mediated by the CB2 receptor in prostate tumor cell lines and did not affect the CB1 receptor [26], thus being not much affine to the CB1 receptor should not induce the psychoactive side effects due to the CB1 receptor activation. We previously used VL15 in cell viability assays to test its effects in several tumor cell line, breast cancer cells, prostate cancer cells, glioblastoma cells and gastric adenocarcinoma cells. VL15 showed a relatively potent inhibitory effect in these cell lines, the highest effect was observed in gastric adenocarcinoma cells [26]. In the present study, we observed that VL15 blocked the proliferative response of MBP activated PBMC and the production of TNF- $\alpha$  in a dose dependent manner. The inhibitory effect of TNF- $\alpha$  is of particular interest, because this cytokine is usually enhanced in

autoimmune pathologies like MS, characterized by autoreactive lymphocytes. Furthermore, in order to assess if the effect of VL15 could be observed also in cells deficient of cannabinoid receptors, we used CHO cells that do not express these receptors. Interestingly, VL15 did not affect CHO cell viability. These data further suggest VL15 cannabinoid receptor selectivity. To establish if the anti-proliferative effect on PBMC could be ascribed to cell death, we evaluated cell viability and observed that VL15 only slightly reduced the number of activated vital cells at the highest concentration. Thus, for the following assays the concentration of 10 $\mu$ M was used, as also previous studies suggested that micromolar doses of synthetic CB2 ligands are used to observe efficacy in the modulation of immune cell function [27]. Then, we investigated in PBMC the effect of VL15 on cell cycle progression. As expected, VL15 treatment reduced the number of cells in the S phase of the cycle this result correlates with the block of the proliferative response as consequence of DNA synthesis inhibition observed in Fig. 2A. Indeed, the enhanced subG0 phase observed in the presence of VL15 indicative of cell death, is in agreement with the slight inhibition of cell vitality observed in Fig. 4. Thus, VL15 interfere with the cell cycle of activated PBMC. Cell activation is a hallmark of MS and adhesion molecules are critical players in the regulation of transmigration of blood leukocytes across the BBB in MS. Interestingly, VL15 was particularly efficient to decrease cell activation markers like CD69, CD54 adhesion molecule and CD49d integrin on CD4<sup>+</sup>T cells. This finding correlates with our previous study, showing that another naphthyridine compound, CB74, was able to reduce cell activation and adhesion [27]. It is known that the down-regulation of adhesion molecules by cannabinoid agonists interferes with the progression of autoimmune diseases like MS [39], thus suggesting a therapeutic benefit derived by the use of modulators of these molecules. To explore the signaling pathways involved in the effects of VL15, we analyzed the expression of some relevant proteins. Of note, VL15, down-regulated the expression level of the phosphorylated NF-kB, IKK $\alpha$  $\beta$ , phosphorylated ERK and Akt with respect to MBP activated cells in which, as expected, we observed increase of NF-kB phosphorylation as consequence of IKK kinase activation as well as up-regulation of ERK and Akt phosphorylation. Our further investigation showed that VL15 has high intestinal absorption properties and might have good ability to cross the BBB by passive diffusion; these data suggest that it might be potentially active on infiltrating lymphocytes in the CNS. Another common feature of MS is the infiltration of auto-reactive leucocytes at the site of inflammation. Current approaches to contrast this disease consist of targeting the CB2 receptor that has been shown to exhibit a protective role in MS, given the psychotropic effects ascribed to the activation of the CB1

receptor. The passage of CB2 receptor ligands through BBB could be desirable to likely keep their benefic properties also on infiltrated lymphocytes in the CNS.

The calculated physicochemical properties and the results of drug-permeability assays in Caco-2 and MDCK cells for VL15, highlight potential therapeutic utility of this compound in diseases like MS.

### **Acknowledgments**

This study was supported by FISM -Fondazione Italiana Sclerosi Multipla – Cod. 2009/R/3/C1

A.M.M. was supported by a fellowship from FISM -Fondazione Italiana Sclerosi Multipla.

### **Conflict of interest**

The authors declare that they have no conflict of interest.

### **References**

- [1] Matsuda LA, Lolait SJ, Brownstein MJ, Young AC, Bonner TI. Structure of a cannabinoid receptor and functional expression of the cloned cDNA. *Nature* 1990; 346: 561–4.
- [2] Howlett AC, Barth F, Bonner TI, Cabral G, Casellas P, Devane WA et al. International Union of Pharmacology. XXVII. Classification of cannabinoid receptors. *Pharmacol Rev* 2002; 54: 161–202.
- [3] Pryce G, Ahmed Z, Hankey DJ, Jackson SJ, Croxford JL, Pocock JM et al. Cannabinoids inhibit neurodegeneration in models of multiple sclerosis. *Brain* 2003; 126 (Pt 10): 2191-202.
- [4] Jackson SJ, Pryce G, Diemel LT, Cuzner ML, Baker D. Cannabinoid-receptor 1 null mice are susceptible to neurofilament damage and caspase 3 activation. *Neuroscience* 2005; 134 (1): 261-8.
- [5] Loría F, Petrosino S, Hernangómez M, Mestre L, Spagnolo A, Correa F et al. An endocannabinoid tone limits excitotoxicity in vitro and in a model of multiple sclerosis. *Neurobiol Dis.* 2010; 37(1): 166-76.
- [6] Klein TW, Newton C, Larsen K, Lu L, Perkins I, Nong L et al. The cannabinoid system and immune modulation. *J Leukoc Biol.* 2003; 74(4): 486-96.
- [7] Van Sickle MD, Duncan M, Kingsley PJ, Mouihate A, Urbani P, Mackie K, et al. Identification and functional characterization of brainstem cannabinoid CB2 receptors. *Science* 2005; 310 (5746): 329-32.

- [8] Maresz K, Carrier EJ, Ponomarev ED, Hillard CJ, Dittel BN. Modulation of the cannabinoid CB2 receptor in microglial cells in response to inflammatory stimuli. *J Neurochem*. 2005; 95 (2): 437-45.
- [9] Gong JP, Onaivi ES, Ishiguro H, Liu QR, Tagliaferro PA, Brusco A et al. Cannabinoid CB2 receptors: immunohistochemical localization in rat brain. *Brain Res* 2006; 1071 (1):10-23.
- [10] Rossi F, Siniscalco D, Luongo L, De Petrocellis L, Bellini G, Petrosino S, et al. The endovanilloid/endocannabinoid system in human osteoclasts: possible involvement in bone formation and resorption. *Bone* 2009; 44(3):476-84
- [11] Bifulco M, Laezza C, Malfitano AM. From anecdotal evidence of cannabinoids in multiple sclerosis to emerging new therapeutical approaches. *Mult Scler* 2007; 13(1): 133-4.
- [12] Bifulco M, Malfitano AM, Pisanti S, Laezza C. Endocannabinoids in endocrine and related tumours. *Endocr Relat Cancer*. 2008;15(2):391-408.
- [13] Malfitano AM, Ciaglia E, Gangemi G, Gazzero P, Laezza C, Bifulco M. et al. Update on the endocannabinoid system as an anticancer target. *Expert Opin Ther Targets* 2011; 15(3): 297-308.a
- [14] Hillard CJ, Weinlander KM, Stuhr KL Contributions of endocannabinoid signaling to psychiatric disorders in humans: genetic and biochemical evidence. *Neuroscience* 2012; 204:207-29.
- [15] Sospedra M, Martin R. Immunology of multiple sclerosis. *Annu Rev Immunol* 2005; 23: 683-747.
- [16] Malfitano AM, Matarese G, Pisanti S, Grimaldi C, Laezza C, Bisogno T et al. Arvanil inhibits T lymphocyte activation and ameliorates autoim-mune encephalomyelitis. *J Neuroimmunol* 2006; 171(1-2): 110-9.
- [17] Malfitano AM, Proto MC, Bifulco M. Cannabinoids in the management of spasticity associated with multiple sclerosis. *Neuropsychiatr Dis Treat* 2008; 4(5): 847-53.
- [18] Cabral and Griffin-Thomas. Emerging role of the cannabinoid receptor CB2 in immune regulation: therapeutic prospects for neuroinflammation. *Expert Rev Mol Med*. 2009; 20;11:e3.
- [19] Zhang M, Martin BR, Adler MW, Razdan RJ, Kong W, Ganea D et al. Modulation of cannabinoid receptor activation as a neuroprotective strategy for EAE and stroke. *J Neuroimmune Pharmacol* 2009; 4(2):249-59.
- [20] Mestre L, Docagne F, Correa F, Loría F, Hernangómez M, Borrell J et al. A cannabinoid agonist interferes with the progression of a chronic model of multiple sclerosis by downregulating adhesion molecules. *Mol Cell Neurosci*. 2009;40(2):258-66.

- [21] Pertwee RG. Emerging strategies for exploiting cannabinoid receptor agonists as medicines. *Br J Pharmacol* 2009; 156(3): 397-411.
- [22] Manera C, Benetti V, Castelli MP, Cavallini T, Lazzarotti S, Pibiri F et al. Design, synthesis, and biological evaluation of new 1,8-naphthyridin-4(1H)-on-3-carboxamide and quinolin-4(1H)-on-3-carboxamide derivatives as CB2 selective agonists. *J Med Chem* 2006; 49(20): 5947–57.
- [23] Manera C, Cascio MG, Benetti V, Allarà M, Tuccinardi T, Martinelli A et al. New 1,8-naphthyridine and quinoline derivatives as CB2 selective agonists. *Bioorg Med Chem Lett* 2007; 17(23): 6505-10.
- [24] Ferrarini PL, Calderone V, Cavallini T, Manera C, Saccomanni G, Pani L et al. Synthesis and biological evaluation of 1,8-naphthyridin-4(1H)-on-3-carboxamide derivatives as new ligands of cannabinoid receptors. *Bioorg Med Chem* 2004; 12 1921-33.
- [25] Manera C, Saccomanni G, Adinolfi B, Benetti V, Ligresti A, Cascio MG et al. Rational design, synthesis, and pharmacological properties of new 1,8-naphthyridin-2(1H)-on-3-carboxamide derivatives as highly selective cannabinoid-2 receptor agonists. *J Med Chem* 2009; 52(12): 3644-51.
- [26] Manera C, Saccomanni G, Malfitano AM, Bertini S, Castelli F, Laezza C et al. Rational design, synthesis and anti-proliferative properties of new CB2 selective cannabinoid receptor ligands: An investigation of the 1,8-naphthyridin-2(1H)-one scaffold. 2012; *Eur J Med Chem* 52:284-94.
- [27] Malfitano AM, Laezza C, D'Alessandro A, Procaccini C, Saccomanni G, Tuccinardi T et al. Effects on Immune Cells of a New 1,8-Naphthyridin-2-One Derivative and Its Analogues as Selective CB2 Agonists: Implications in Multiple Sclerosis. *PLoS One*. 2013; 8(5):e62511
- [28] Malfitano AM, Laezza C, Saccomanni G, Tuccinardi T, Manera C, Martinelli A, et al. Immune-Modulation and Properties of Absorption and Blood Brain Barrier Permeability of 1,8-Naphthyridine Derivatives. *J Neuroimmune Pharmacol*. 2013. 8(5):1077-86.
- [29] Fulp A, Bortoff K, Seltzman H, Zhang Y, Mathews J, Snyder R et al. Design and synthesis of cannabinoid receptor 1 antagonists for peripheral selectivity, *J Med Chem*. 2012; 55(6):2820-28 34.
- [30] Benavides A, Napolitano A, Bassarello C, Carbone V, Gazerro P, Malfitano A et al. Oxylipins from *Dracontium lorentense*. *J Nat Prod* 2009; 72(5):813-7.

- [31] Malfitano AM, Sosa S, Laezza C, De Bortoli M, Tubaro A, Bifulco M. Rimonabant reduces keratinocyte viability by induction of apoptosis and exerts topical anti-inflammatory activity in mice. *Br J Pharmacol* 2011; 162(1): 84-93.b
- [32] Santoro A, Pisanti S, Grimaldi C, Izzo AA, Borrelli F, Proto MC et al. Rimonabant inhibits human colon cancer cell growth and reduces the formation of precancerous lesions in the mouse colon. *Int J Cancer*. 2009; 125(5):996-1003.
- [33] *QikProp*, version 3.2, Schrodinger, Inc.: New York, 2007.
- [34] Tetko I V, Gasteiger J, Todeschini R, Mauri A, Livingstone D, Ertl P et al. Virtual computational chemistry laboratory - design and description, *J Comput Aid Mol Des*. 2005; 19(6):453-463
- [35] *Macromodel*, version 8.5; Schrodinger, Inc.: New York, 1999.
- [36] Jönsson S, Andersson G, Fex T, Fristedt T, Hedlund G, Jansson K et al. Synthesis and biological evaluation of new 1,2-dihydro-4-hydroxy-2-oxo-3-quinolinecarboxamides for treatment of autoimmune disorders: structure-activity relationship. *J Med Chem*. 2004; 47(8):2075–2088.
- [37] Jansson K, Fristedt T, Olsson A, Svensson B, Jönsson, S. Synthesis and reactivity of laquinimod, a quinoline-3 carboxamide: intramolecular transfer of the enol proton to a nitrogen atom as a plausible mechanism for ketene formation. *J Org Chem*. 2006; 71(4):1658–1667.
- [38] Mugnaini C, Brizzi A, Ligresti A, Allarà M, Lamponi S, Vacondio F, et al. Investigations on the 4-Quinolone-3-carboxylic Acid Motif. 7. Synthesis and Pharmacological Evaluation of 4-Quinolone-3-carboxamides and 4-Hydroxy-2-quinolone-3-carboxamides as High Affinity Cannabinoid Receptor 2 (CB2R) Ligands with Improved Aqueous Solubility. *J Med Chem*. 2016;59(3):1052-1067.
- [39] Mestre L, Docagne F, Correa F, Lori'a F, Hernango'mez M, Borrel J, et al. (2009) A cannabinoid agonist interferes with the progression of a chronic model of multiple sclerosis by downregulating adhesion molecules. *Mol Cell Neurosci*. 40(2): 258–66.

## Figure Legends

### Figure 1

*VL15 chemical structure.*

In Fig. 1 the chemical structure of VL15 is reported.

## Figure 2

*VL15 inhibits proliferation of MBP activated PBMC and TNF- $\alpha$  production.*

MBP activated PBMC were treated with VL15 at the indicated concentrations from 10  $\mu$ M to 0.3  $\mu$ M in triplicate. The counts per minutes (c.p.m.)  $\pm$  the standard deviation of the triplicates of a representative experiment out of five are shown (A). The mean percent of inhibition of cell proliferation elicited by VL15 at the concentration of 10  $\mu$ M of all the independent experiments performed is 93,8% $\pm$ 6,1. The statistical significance of VL15 inhibitory effect was calculated with respect to the MBP activated cells (\*p<0.05, §p<0.01). The histogram B represents the effect of VL15 used at 10 $\mu$ M and 3  $\mu$ M on TNF- $\alpha$  secretion in cell supernatant of PBMC activated with MBP. The mean percent of inhibition of TNF- $\alpha$  production exhibited by VL15 at the concentration of 10  $\mu$ M of all the independent experiments performed is 91,4% $\pm$ 2,1. The inhibitory effect was calculated with respect to MBP-activated PBMC, (MBP in the figures) (\*p<0,05). The histograms reported show a single experiment representative of four independent experiments with reproducible results.

## Figure 3

*VL15 does not affect CHO cell viability.*

CHO cells were treated with VL15 at the indicated concentrations from 10  $\mu$ M to 0.3  $\mu$ M in triplicate. Optical density (O.D.) of the triplicates of a representative experiment out of three is shown. VL15 did not affect cell viability with respect to non-treated cells (CTR).

## Figure 4

*VL15 slightly reduces PBMC viability.*

MBP activated PBMC were treated with VL15 at the concentration of 10 $\mu$ M and cultured for 6 days. After the incubation, cells were collected, stained with trypan blue and counted. The percent of cell viability was evaluated on PBMC, MBP activated PBMC and in the presence and in the absence of VL15 (10 $\mu$ M). The histogram reported, shows the percent of live cells in PBMC, MBP activated PBMC (MBP in the figure) and in the presence of VL15. The inhibitory effect of VL15 was calculated with respect to MBP-activated PBMC, (MBP in the figures) (\*p<0,05).

The histogram is representative of four independent experiments. The mean percent of inhibition of cell viability elicited by VL15 at the concentration of 10  $\mu$ M of all the independent experiments performed is 30,2% $\pm$ 5,2.

### **Figure 5**

*Effects of VL15 on cell cycle progression.*

In this figure the cell cycle progression of MBP activated PBMC treated with VL15 (10 $\mu$ M) is reported. The bars in the histogram are calculated as mean of three independent experiments and represent on the y axe, the percent of cells in each phase of the cell cycle. The statistically significant increase of the subG0 phase and the decrease of the S and G2/M phases (\*p<0.05) following treatment with VL15 are illustrated in the figure and are calculated with respect to MBP activated cells.

### **Figure 6**

*Effect of VL15 on T cell activation markers.*

MBP activated PBMC were treated with the drug at the concentration of 10 $\mu$ M and cultured for 6 days. After the incubation, cells were collected and stained with the antibodies indicated in the figure. Cells were analyzed by flow cytometry gating on the lymphocyte region of CD4+T cells. In the histogram, the inhibitory effect of VL15 on cells expressing CD69, CD49d, CD54 and CD25 is reported considering as control untreated MBP activated cells (0% of inhibition). The histogram reports the mean percent of marker inhibition  $\pm$  standard deviation of four independent experiments. The statistical analysis was performed on four experiments (\*p<0,05 calculated with respect to MBP activated cells).

### **Figure 7**

*VL15 controls NF- $\kappa$ B, IKK $\alpha\beta$ , IKK $\alpha$ , Akt and ERK expression.*

Western blot and densitometric analysis of total and phosphorylated NF- $\kappa$ B, IKK $\alpha\beta$ , IKK $\alpha$ , Akt and ERK proteins are reported in the presence of VL15 (10 $\mu$ M) along with the controls PBMC and MBP activated PBMC (MBP in the figure). The blots are representative of three independent experiments.